

## Boreal–Tethyan Correlation of the Jurassic–Cretaceous Boundary Interval by Magneto- and Biostratigraphy

V. Houša<sup>†a</sup>, P. Pruner<sup>a</sup>, V. A. Zakharov<sup>b</sup>, M. Kostak<sup>c</sup>, M. Chadima<sup>a</sup>, M. A. Rogov<sup>b</sup>, S. Šlechtá<sup>a</sup>, and M. Mazuch<sup>c</sup>

<sup>a</sup> Czech Academy of Sciences, Prague

<sup>b</sup> Geological Institute of RAS, Moscow

<sup>c</sup> Charles University, Prague

Received October 31, 2006

**Abstract**—As a result of detail sampling and paleomagnetic study of the 27-m-thick section of Jurassic–Cretaceous boundary beds in the Nordvik Peninsula (Anabar Bay, Laptev Sea), a succession of M-zones correlative with chrons M20n–M17r is established for the first time in the Boreal deposits. Inside the normal polarity zone corresponding to Chron M20n, a thin interval of reversed polarity, presumably an equivalent of the Kysuca Subzone (M20n.1r), is discovered. The other thin interval of reversed polarity established within the next normal polarity zone (M19n) is correlated with the Brodno Subzone (M19n.1r). The same succession of normal and reversed polarity zones has been discovered recently in the Jurassic–Cretaceous boundary beds of the Tethyan sections: in the Bosso Valley (Italy), at the Brodno (Slovak Republic) and Puerto Escaño (Spain) sites. Correlation of successions established lead us to conclusion, that the Jurassic–Cretaceous boundary corresponds in the Panboreal Superrealm to a level within the *Craspedites taimyrensis* Zone of the upper Volgian Substage. Hence, the greatest part of Volgian Stage should be included into the Jurassic System. Biostratigraphic data do not contradict this conclusion.

**DOI:** 10.1134/S0869593807030057

**Key words:** Jurassic–Cretaceous boundary, Boreal and Tethyan deposits, magnetostratigraphy, biostratigraphy, Northern Siberia.

### INTRODUCTION

Climatic zoning and some paleoceanographic peculiarities, which existed during the Late Jurassic and Early Cretaceous in the Northern Hemisphere, were responsible for a significant difference in taxonomic composition of marine and terrestrial biota on the north and south, i.e., in the northern Panboreal and southern Tethys–Panthalassa superrealms. Especially sharp distinctions between biotas of these superrealms were characteristic of the terminal Jurassic and initial Cretaceous. This is the main reason that complicates a detailed biostratigraphic correlation between the Jurassic–Cretaceous boundary beds of the Boreal and Tethyan types. Many versions of zone-by-zone correlation between the Tithonian and Berriasian stages in the south and the Volgian and Ryazanian stages in the north, respectively, have been suggested by researchers during last 50 years, but none of them is unanimously substantiated. Hitherto, it was impossible to use independent paleomagnetic method in addition to micro- and macropaleontological approach for correlation of the Jurassic–Cretaceous boundary beds in two superrealms, because there were no valid paleomagnetic data

for the Volgian and Ryazanian stages. In order to overcome this difficulty, we undertook in 2003–2006 a joint bio- and magnetostratigraphic study of the Jurassic–Cretaceous boundary beds in the Nordvik peninsula, North Siberia (Fig. 1). This stratigraphically continuous section of Upper Volgian and Ryazanian sediments is exposed along west coast of the Anabar Bay (Laptev Sea). Zones of ammonites and bachiids established here earlier (Zakharov et al., 1983) has been substantiated once again during fieldworks of 2003 with the only one significant change in biostratigraphy: the recent correlation between the middle–upper Volgian boundary beds of the Russian Platform and North Siberia showed that *Exoticus* Zone should belong to the middle not the upper Volgian Substage (Zakharov and Rogov, 2006). The studied section (Fig. 2) consists of marine silty-clayey deposits with abundant concretions and few carbonate interlayers cemented during the early diagenesis. The key interval 27 m thick has been determined for paleomagnetic sampling based on biostratigraphic data characterizing the topmost middle Volgian (*Epivirgatites variabilis* Zone) and lowermost Ryazanian (*Hectoroceras kochi* Zone). As a result, we managed to suggest for the first time a well-substantiated version of magnetostratigraphic correlation between

<sup>†</sup> Deceased.

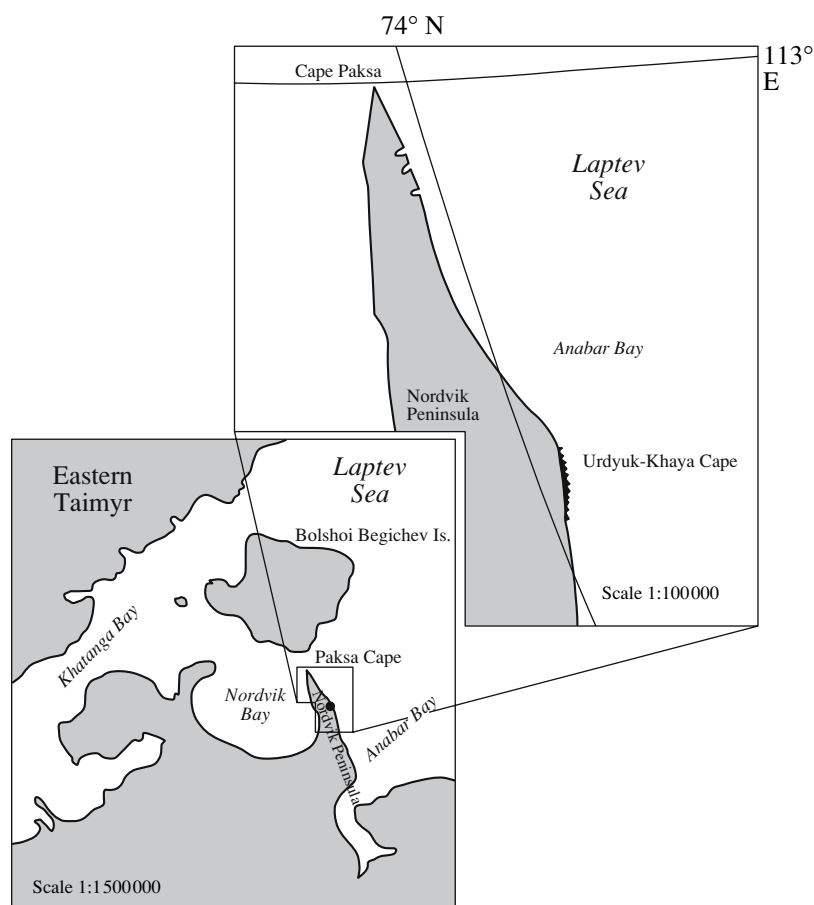


**Fig. 1.** Location map of the section studied, the Urdyuk-Khaya Cape, Nordvik Peninsula, western coast of Anabar Bay of Laptev Sea.

the Jurassic–Cretaceous boundary beds of South Europe and that distant region of North Siberia. The new results obtained are consistent with biostratigraphic evidences.

#### PALEOMAGNETIC STUDY

This study is continuation of a joint geophysical and paleontological project aimed at detailed magnetostratigraphic and paleontological investigation of the Jurassic–Cretaceous boundary strata. The project objective is to establish correlation between biozones in this stratigraphic interval in the Tethys–Panthalassa and Panboreal Superrealms using global paleomagnetic events (Houša et al., 1999, 2000).

Oriented samples have been collected from 370 stratigraphic levels of three individual sections (Fig. 2). Sections H and D are respectively above and below the supposed Jurassic–Cretaceous boundary in the boreal scale. This boundary is marked by a 4- to 6-cm-thick horizon of phosphate limestone enriched in iridium and other noble metals (Zakharov et al., 1993). Because of a fault zone, continuation of section D (designated as section M) was sampled a few hun-

dreds meters apart from section D. Simultaneously we sampled rocks from approximately 2-m-thick overlapping interval between sections D and M to ensure correctness of their correlation (Fig. 2). Letters in sample numbers indicate relevant sections and numeral parts correspond to the sampling level distance in cm from the supposed Jurassic–Cretaceous boundary. In the middle part of the section, sampling intervals range from 2 to 4 cm (D section), being up to 10 cm wide near the base and top of the sampled sequence (sections H and M).

The Natural Remanent Magnetization (NRM) has been studied to determine the magnetic polarity and to solve problems of magnetostratigraphy. Progressive stepwise demagnetization in alternating field (AF) up to maximum of 100 mT was performed using 2 G Enterprises degausser system. After each demagnetization step, the NRM was measured on 2 G Enterprises cryogenic magnetometer at the Geological Research Center, Potsdam, Germany. The measured data were subjected to the multi-component analysis of remanence (Kirschvink, 1980). After AF treatment all the samples were successfully demagnetized usually to less than 1% of the original NRM value. The mean direc-

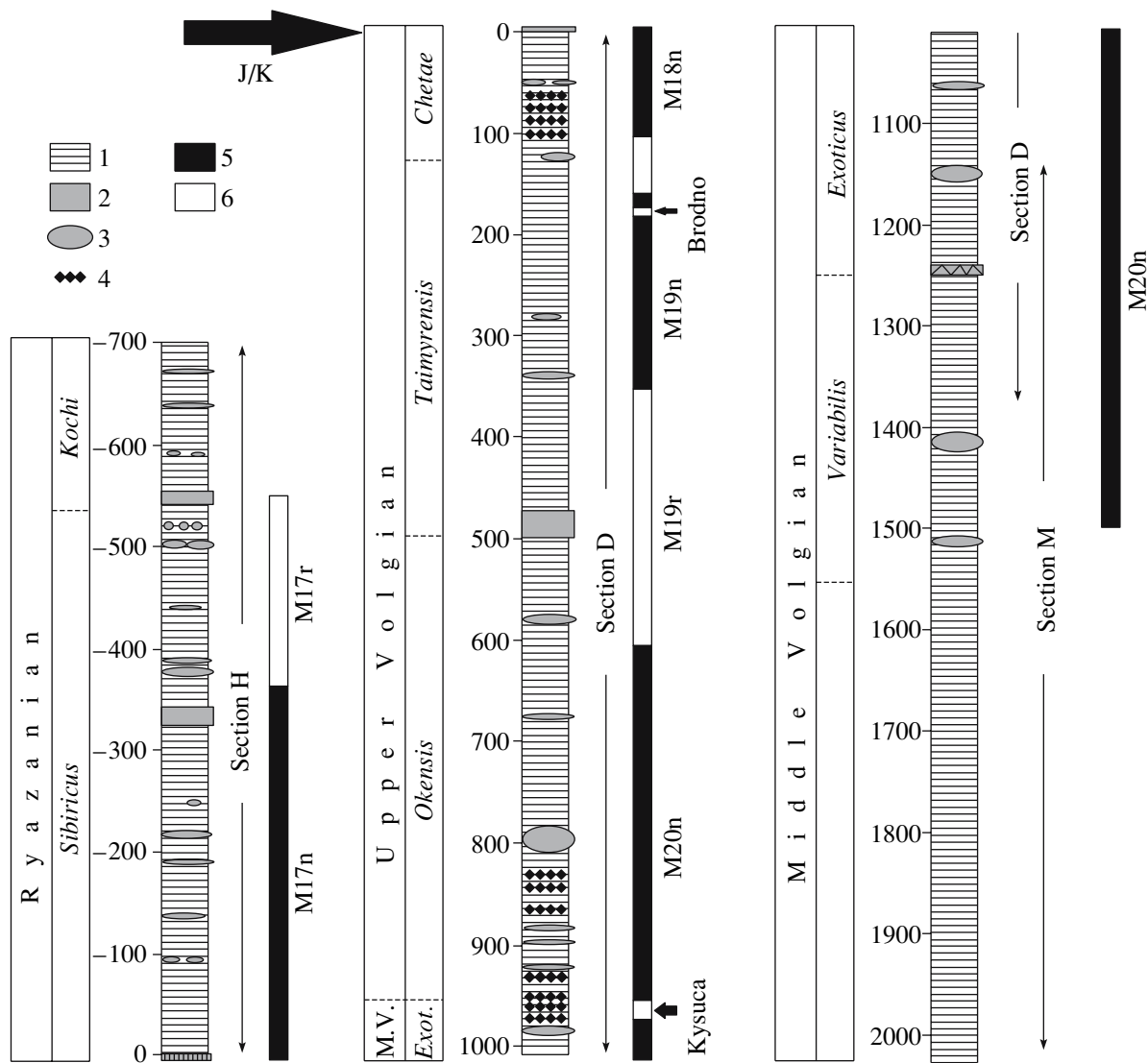


**Fig. 2.** Lithostratigraphy of the studied sections and sampling intervals for paleomagnetic analysis (magneto- and biostratigraphic units are shown to the right and left, respectively, of lithologic columns: (1) clay-silty rocks; (2) beds with siderite cement; (3) siderite nodules; (4) pyrite segregations or interlayers; (5) intervals of normal and (6) reverse polarity; (M. V.) middle Volgian Substage; (*Exot.*) *Exoticus* Zone

tions of Characteristic Remanent Magnetization (ChRM) were analyzed using the statistics on sphere (Fisher, 1953). Approximately 85% of all the samples from the studied section belong to the group of rocks, which recorded two magnetic components of high coercivity ChRM (high field resistant).

Chadima et al. (2006) already published interpretation of magnetomineralogic analyses of rocks selected for paleomagnetic investigation. In this work, we analysed magnetic susceptibility ( $k$ ) and natural remanent magnetization (NRM) as dependent on temperature and obtained hysteretic parameters of rocks. An integrated magnetic fabric approach (AMS, high-field anisotropy, anisotropy of anhysteretic remanent magnetization) has been combined with standard magnetic and non-magnetic mineral identification techniques.

The understanding of mineralogical control on magnetic fabric has been used to discriminate samples unsuitable for a reliable magnetostratigraphic interpretation.

The magnetic susceptibility ( $k$ ) ranges from  $1 \times 10^{-5}$  to  $30 \times 10^{-5}$  SI and is predominantly controlled by paramagnetic minerals, i.e., by ironbearing chlorites, micas, and siderite. The siderite-bearing samples possess the highest magnetic susceptibility up to  $70 \times 10^{-5}$  that likely points to presence of dispersed microscopic magnetite grains commonly associated with siderite.

The NRM intensity varies between  $5 \times 10^{-5}$  and  $2 \times 10^{-3}$  A/m. Several samples with extremely high NRM values ( $> 5 \times 10^{-3}$  A/m) apparently contain authigenic magnetite that is evident from a sharp susceptibility decrease at approximately 550°C.

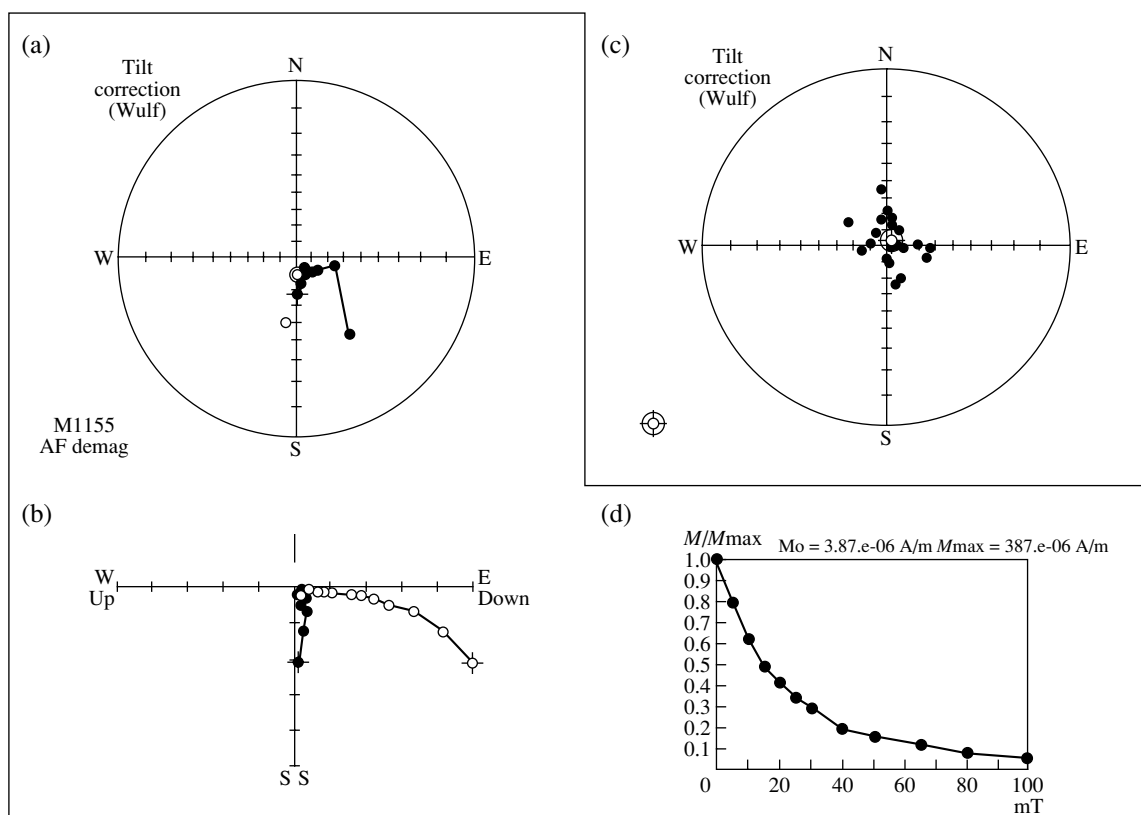


**Fig. 3.** Results of AF demagnetization of siderite-bearing samples: (a) Stereographic projection of NRM vector variations during AF demagnetization, solid and open circles denote projections of NRM vectors on the lower and upper hemispheres respectively; (b) Zijderveld diagram, solid circles denote projection on horizontal plane (XY), open circles on the N–S vertical plane (XZ); (c) stereographic projection of NRM vectors after demagnetization; (d) NRM module (M) as dependent on AF intensity; (1) mean vector direction and confidence circle (95% probability level).

Susceptibility resolution into paramagnetic and ferromagnetic components showed that  $k$  variations are almost entirely controlled by paramagnetic components.

According to magnetomineralogic analyses, three different groups of samples can be distinguished (Chadima et al., 2006). The first group includes samples with the highest magnetic susceptibility and relatively low NRM values. In the studied sections, these high- $k$  samples usually characterize concretions and cemented layers, in which siderite can be macroscopically observed sometimes. After AF demagnetization of samples bearing siderite in majority, two NRM components can be isolated (Fig. 3): the components unstable in demagnetizing field of approximately 5–15 mT and the other ones stable in the field of 15–80 mT. The latter can be interpreted as the Characteristic Remanent Magnetization (ChRM). The mean ChRM directions in geographic and stratigraphic coordinates (before and after tilt correction) are given in Table 1. Only the normal magnetic polarity is established for all the siderite-bearing samples (Fig. 3). Although the siderite-bearing samples could be magnetized during diagenesis of sediments, absence of the reversed polarity is suggestive of remagnetization.

Triaxial-fabric samples of the second group reveal the highest NRM and relatively low  $k$  values. After AF demagnetization, only one NRM component unstable in demagnetizing field of 5–80 mT can be isolated (Fig. 4). Paleomagnetic directions of normal and reversed polarities are highly scattered in this case (Table 2), and the ChRM isolated from the high-NRM samples cannot be used for magnetostratigraphic interpretation.

According to results magnetic fabric and paleomagnetic component analyses, we exclude the siderite-bearing and high-NRM samples (about 15% of all the samples) from further magnetostratigraphic considerations (Chadima et al. 2006).

The third group is represented by the black shale samples representing approximately 85% of the analyzed collection. Magnetic anisotropy of these rocks is controlled predominantly by the preferred orientation of iron-bearing chlorites or micas, and, to a minor extent, by ferromagnetic fraction (Chadima et al., 2006). Typical examples of AF demagnetization diagrams obtained for black shales sampled from different polarity zones and having different NRM values are shown in Figs. 5, 6 and 7. The samples display a well-

**Table 1.** Siderite: mean directions of remanence C-components after and before structural tilt correction ( $\alpha_{95}$  is confidence circle radius at the 95% probability level;  $k$  paleomagnetic concentration;  $n$  number of samples)

| Rock     | Component of remanence | Polarity | After structural tilt correction |                 |                   |      | Before structural tilt correction |                 |                   |      | $n$ |
|----------|------------------------|----------|----------------------------------|-----------------|-------------------|------|-----------------------------------|-----------------|-------------------|------|-----|
|          |                        |          | mean direction                   |                 | $\alpha_{95}$ [°] | $k$  | mean direction                    |                 | $\alpha_{95}$ [°] | $k$  |     |
|          |                        |          | declination [°]                  | inclination [°] |                   |      | declination [°]                   | inclination [°] |                   |      |     |
| Siderite | C                      | N        | 46.5                             | 86.5            | 6.3               | 21.6 | 92.1                              | 65.0            | 8.7               | 11.2 | 23  |

See Fig. 3

**Table 2.** High NRM rocks (>5 mA/m): mean directions of B-components of remanence after and before structural tilt correction (symbols as in Table 1)

| Rock     | Component of remanence | Polarity | After structural tilt correction |                 |                   |     | Before structural tilt correction |                 |                   |     | $n$ |
|----------|------------------------|----------|----------------------------------|-----------------|-------------------|-----|-----------------------------------|-----------------|-------------------|-----|-----|
|          |                        |          | mean direction                   |                 | $\alpha_{95}$ [°] | $k$ | mean direction                    |                 | $\alpha_{95}$ [°] | $k$ |     |
|          |                        |          | declination [°]                  | inclination [°] |                   |     | declination [°]                   | inclination [°] |                   |     |     |
| High NRM | B                      | N        | 152.0                            | 78.2            | 24.1              | 1.8 | 111.9                             | 47.1            | 22.5              | 2.0 | 19  |
| High NRM | B                      | R        | 320.4                            | -61.8           | 25.0              | 2.9 | 300.4                             | -20.8           | 26.4              | 2.5 | 11  |

See Fig. 4

**Table 3.** Black shales: mean directions of C-components of remanence after and before structural tilt correction (symbols as in Table 1)

| Samples     | Component of remanence | Polarity | After structural tilt correction |                 |                   |      | Before structural tilt correction |                 |                   |      | $n$ |
|-------------|------------------------|----------|----------------------------------|-----------------|-------------------|------|-----------------------------------|-----------------|-------------------|------|-----|
|             |                        |          | mean direction                   |                 | $\alpha_{95}$ [°] | $k$  | mean direction                    |                 | $\alpha_{95}$ [°] | $k$  |     |
|             |                        |          | declination [°]                  | inclination [°] |                   |      | declination [°]                   | inclination [°] |                   |      |     |
| Black shale | C                      | N        | 44.9                             | 80.8            | 2.1               | 31.7 | 77.4                              | 59.4            | 3.1               | 12.6 | 174 |
|             | C                      | R        | 281.1                            | -75.6           | 10.1              | 6.7  | 277.2                             | -47.0           | 12.6              | 4.7  | 35  |

See Fig. 8

defined two- to three-component remanence: the A-component of undoubtedly viscous origin can be isolated in the AF range of 0–5 mT; the B-component in the range of 5–15 mT; and the high field C-component in the range of 15–80 mT. The ChRM directions measured with a high precision even for weakly magnetic samples demagnetized to  $5 \times 10^{-6}$  A/m, have been used to detect the normal and reversed polarity zones in the section. The C-component directions corresponding to normal and reverse paleomagnetic polarity in the upper Volgian and Ryazanian black shales are shown in Fig. 8. The mean directions of the remanence C-components estimated in geographic and stratigraphic coordinates (before and after structural tilt correction) are presented in Table 3.

The resulting magnetostratigraphic profile is shown in Fig. 9, being supplemented by variation curves of the NRM modulus ( $M$ ), magnetic susceptibility of samples in natural state ( $k$ ), declination ( $D$ )

and inclination ( $I$ ) of the ChRM, and discriminant function of polarity zones (Man, 2006). Both ChRM directions and calculated pole coordinates (Table 4) are in agreement with relevant parameters characterizing the upper Jurassic and lower Cretaceous sediments in Khatanga River basin (Pospelova, 1971): confidence circle estimated for pole position overlap each other (Table 5).

Six magnetic polarity zones, three of normal (N) and three of reverse (R) polarity, are established in the main interval of the Nordvik section (Fig. 9). In the magnetostratigraphic scale (Ogg and Smith, 2004), magnetostratigraphy of the Jurassic–Cretaceous transition is very complicated, and it is difficult to identify the distinguished polarity zones with standard chrons. Two narrow subzones of reverse polarity, which have been detected in the lower and middle N-zones of the Nordvik section, are important evidences in favor of the section range from Chron M20n to Chron M17r. The

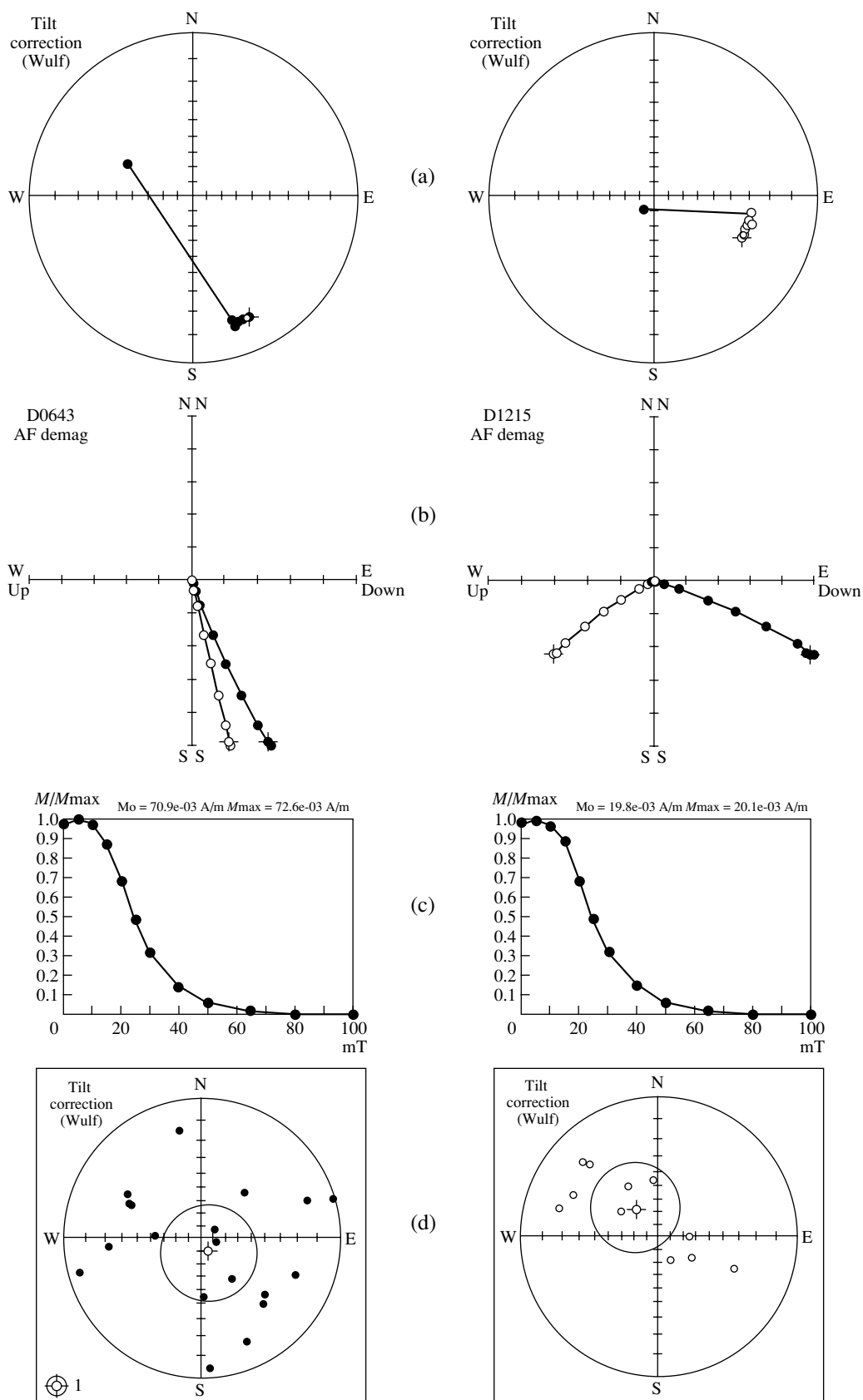


**Fig. 4.** Results of AF demagnetization of two black shale samples with high NRM values (see Fig. 3 caption for explanation to projections A–D).

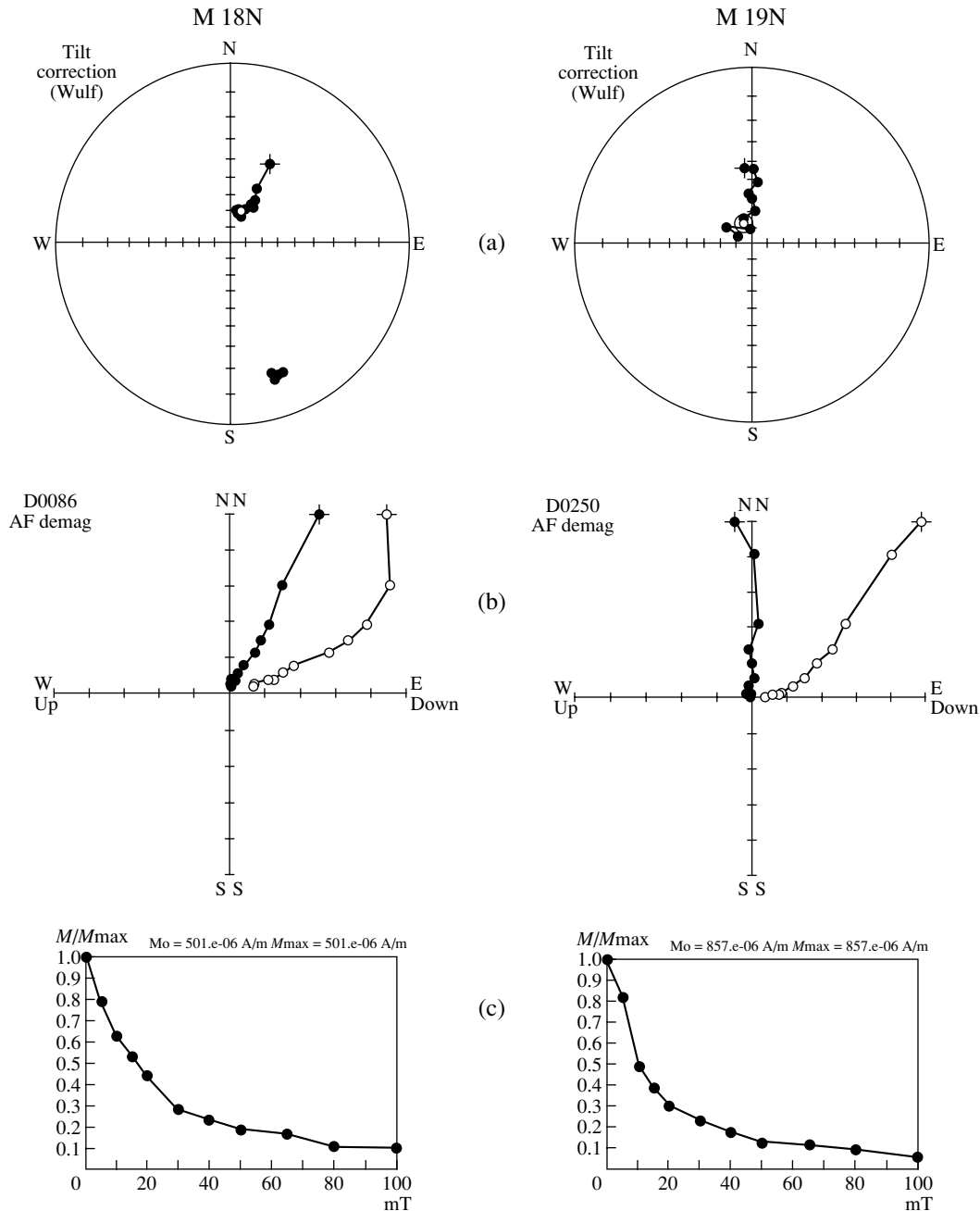


**Fig. 5.** Results of AF demagnetization of two samples from normal polarity zones, the analogs of Chrons M18n and M19n (see Fig. 3 caption for explanation to projections a–c).

analogous narrow R-subzones “Kysuca” and “Brodno” have been distinguished previously within chron M20n and M19n in the Brodno (West Carpathians, Slovakia; Houša et al., 1999), Puerto Escaño (Province of Córdoba, South Spain; Houša et al., 2000), Bosso section (Bosso Valley, Umbria, Central Italy; Houša et al., 2004), being well correlated with succession of marine magnetic anomalies (Ogg and Smith, 2004). Exactly these subzones of reverse polarity substantiate our conclusion that two zones of normal polarity established in

the Nordvik section are correlative with chron M20 and M19.

Presumable analog of the Kysuca Subzone in Chron M20n is only 17 cm thick (Figs. 2 and 9). In the Brodno section (Houša et al., 1999), it is situated above the middle of normal polarity zone M20n. Another interval of reverse polarity correlative with the Brodno Subzone of Chron M19n is 77cm thick.

New magnetostratigraphic data on the Boreal (Arctic) section are compared with magnetostratigraphy of

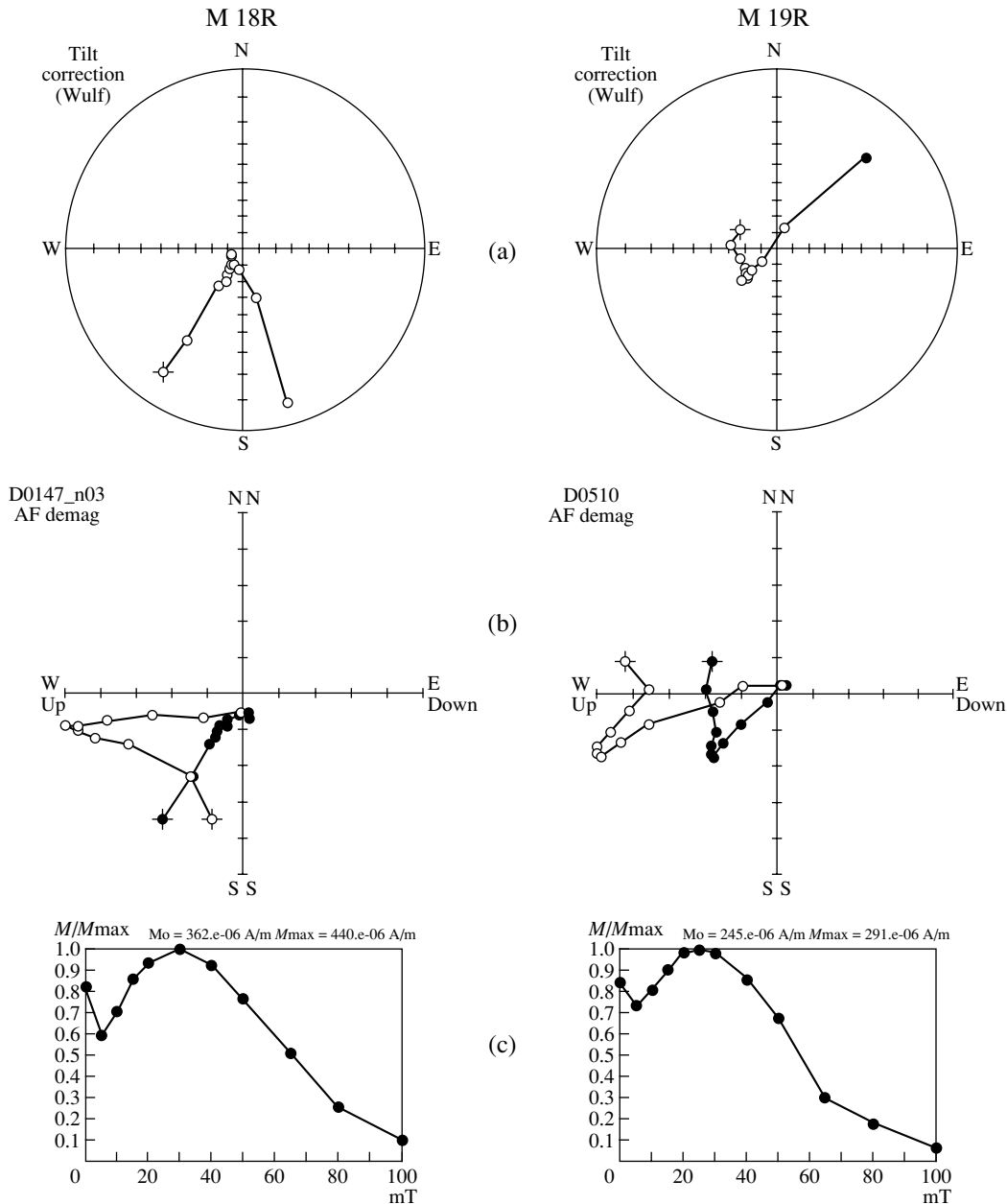


**Fig. 6.** Results of AF demagnetization of two samples from reverse polarity zones, the analogs of Chrons M18r and M19r (see Fig. 3 caption for explanation to projections a–c).

the Jurassic–Cretaceous boundary beds in the Tethyan regions (Fig. 10)

#### STATE-OF-ART OF BIOSTRATIGRAPHICAL CORRELATION

New version of correlation of the Upper Volgian, Upper Tithonian and lowermost Berriasian, supposed on the base of magnetostratigraphic data corresponds very close to traditional zone-by-zone correlation scheme of the Jurassic–Cretaceous boundary (Mesezhnikov, 1989). Inasmuch as *Craspedites taimyrensis*

Zone, within the limits of which the Jurassic–Cretaceous boundary is located according to magnetostratigraphic data, entirely corresponds to *C. nodiger* Zone, hence the former zone of Siberia could be also considered within the Volgian Stage (Shulgina, 1985). Mesezhnikov (1989, p. 105) reasonably suggested just the same version, though reserving possibility of correlation of the overlying zone (correlative with *Subcraspedites (Volgidiscus) maurynjensis* Zone in the Urals), if it will be distinguished in the Russian Platform, with the basal *Jacobi* Zone of the Berriasian). Representatives of subgenus *Volgidiscus* recently have been found



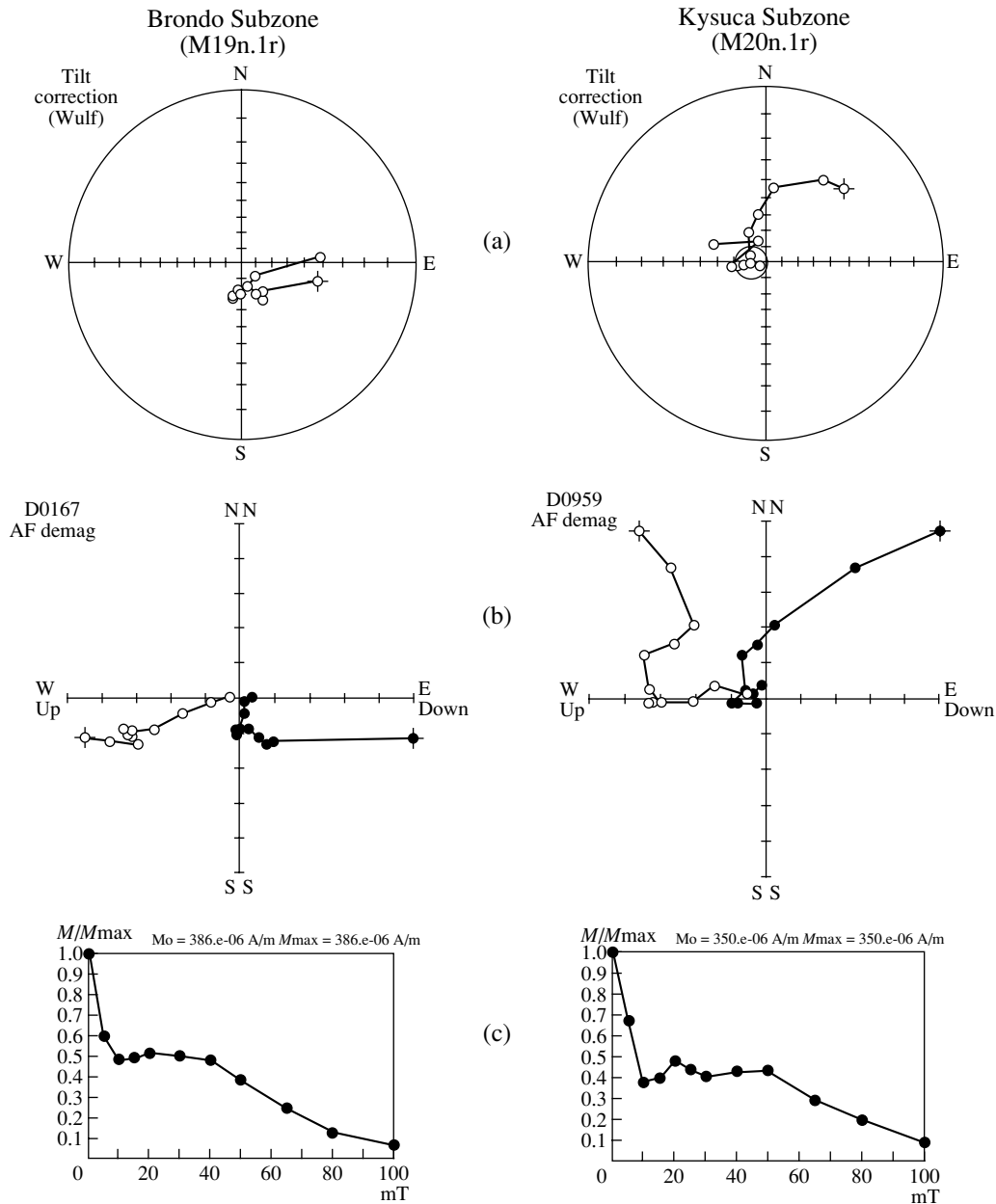


**Fig. 7.** Results of AF demagnetization of two samples from reversed polarity intervals, the analogs of the Brodno (M19n.1r) and Kysuca (M20n.1r) subzones (see Fig. 3 caption for explanation to projections a–c).

at the top of the upper Volgian in the Russian Platform (Kiselev, 2003). Thus *Volgidiscus* Beds fill the gap existed here. Nevertheless, zone-by-zone biostratigraphic correlation of the upper Tithonian and upper Volgian remains provisional due to absence of taxa in common among relevant fossil assemblages. A way out of this situation, Mesezhnikov saw in focusing attention on correlation of the Berriasian base corresponding simultaneously to the Tithonian top (loc. cit., p. 104). However correlation of the Berriasian and Boreal Berriasian (=Ryazanian) still remains ambiguous. New records of the Tethyan and Boreal ammonites in the

lowermost Ryazanian of the Moscow region confirm at least the correlation between the lowermost *Riasanites* Beds (the *Riasanites swistowianus* assemblage) and the *Occitanica* Zone upper part (Mitta, 2006). In opinion of Mitta (2006), below this level there are two additional ammonite assemblages of exceptionally Boreal ammonoids occurring in the same succession as in Arctic areas (*Shulginites–Hectoroceras*). Hence, biostratigraphic data do not define position of the Berriasian base in the Boreal succession. However biostratigraphy certainly proves that the base of the Boreal *Kochi* Zone should be older than upper part of the Tethyan *Occitan-*

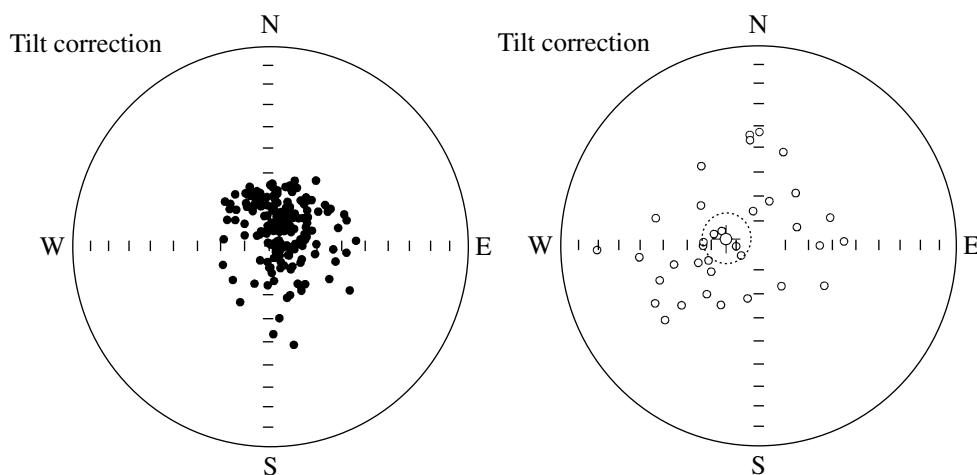


**Fig. 8.** Stereographic projection of ChRM vectors after AF demagnetization black shale samples with normal (left) and reverse (right) polarity (see Fig. 3 caption for explanation to symbols).

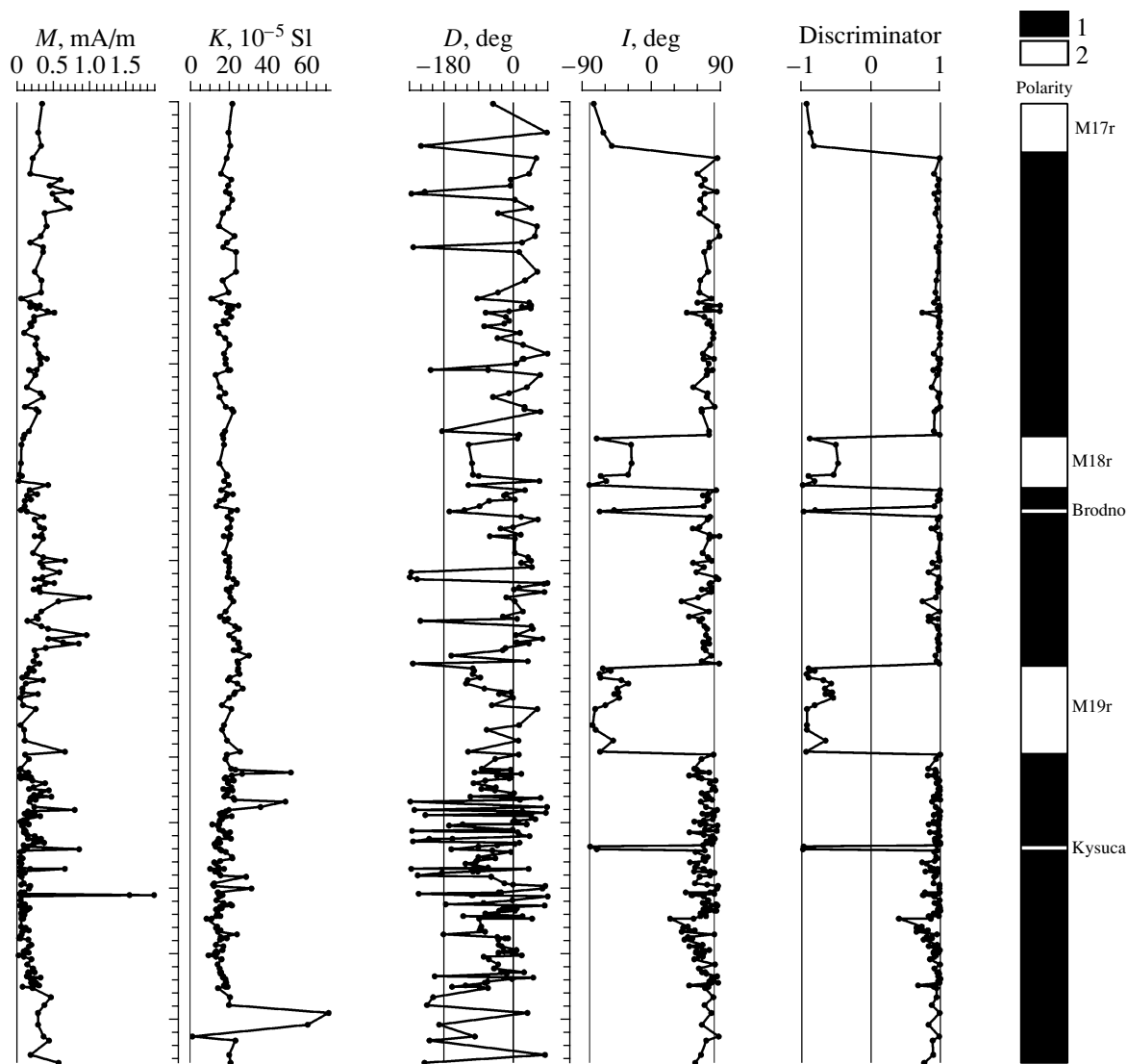


**Fig. 9.** Magnetostratigraphic section of Jurassic–Cretaceous boundary deposits in the Nordvik section (summary of magnetic, paleomagnetic, lithostratigraphic and ammonite data): (*M*) remanent magnetization in the natural state; (*K*) magnetic susceptibility in the natural state; (*D*) declination; (*I*) inclination; (1) intervals of normal and (2) reverse polarity.

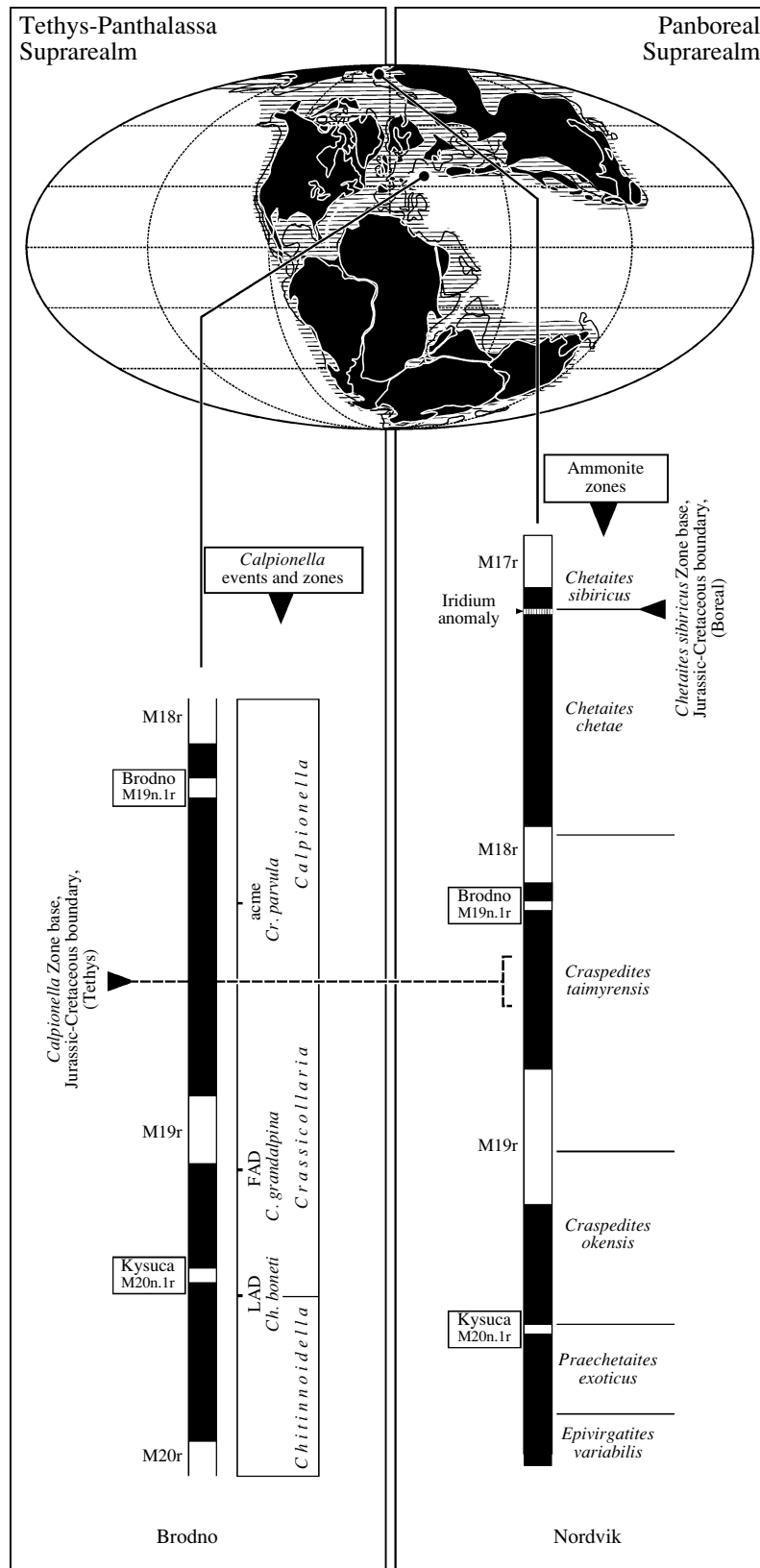


**Fig. 10.** The Boreal-Tethyan paleomagnetic correlation between Jurassic-Cretaceous boundary strata in the Panboreal (Nordvik section) and Tethys-Panthalassa (Brodno section) superrealms (localities of sections are shown in paleogeographic reconstruction after Scotese and Golonka, 1992): (Acme) acme-level; (FAD) first appearance datum; (LAD) last appearance datum.

**Table 4.** Paleomagnetic data for Jurassic–Cretaceous boundary beds of black shales in the Nordvik section (pole coordinates are calculated after rotation of all reverse ChRMs by 180°; symbols as in Table 1)

| Rock                                   | Site coordinates     |                          | Mean paleomag-<br>netic directions |                      | $\alpha_{95}$<br>[°] | $k$  | $n$ | Paleomagnetic<br>pole position |                                 | Ovals of<br>confidence |                |
|--|----------------------|--------------------------|------------------------------------|----------------------|----------------------|------|-----|--------------------------------|---------------------------------|------------------------|----------------|
|  | lat. $\Psi$<br>[°] N | long. $\Lambda$<br>[°] E | declina-<br>tion [°]               | inclina-<br>tion [°] |                      |      |     | paleolat. $\Psi_p$<br>[°] N    | paleolong.<br>$\Lambda_p$ [°] E | $\delta m$ [°]         | $\delta p$ [°] |
| Black shales, after tilt<br>correction | 73.90                | 113.08                   | 48.3                               | 81.7                 | 2.5                  | 16.3 | 209 | 76.9                           | 179.3                           | 4.7                    | 4.8            |

**Table 5.** Paleomagnetic pole positions calculated for Jurassic–Cretaceous boundary beds in North Siberia ( $A_{95}$  is circle of confidence, 95% probability level)

| Region               | Age (Ma) | $A_{95}$ [°] | Paleolatitude<br>$\Psi_p$ [°] N | Paleolongitude<br>$\Lambda_p$ [°] E | References             |
|----------------------|----------|--------------|---------------------------------|-------------------------------------|------------------------|
| Lena River           | 161–100  | 4            | 71                              | 145                                 | Pisarevsky, 1982       |
| Khatanga River basin | 136–133  | 3            | 73                              | 178                                 | Pospelova, 1971        |
| Anabar Bay           | 140–138  | 3            | 63                              | 174                                 | Pospelova et al., 1968 |
| Anabar Bay           | 140–138  | 7            | 64                              | 177                                 | Pospelova et al., 1968 |
| Anabar Bay           | 140–138  | 3            | 64                              | 170                                 | Pospelova et al., 1968 |
| Anabar Bay           | 140–138  | 3            | 62                              | 174                                 | Pospelova et al., 1968 |

ica Zone. This conclusion corresponds well with paleomagnetic results.

### CONCLUSION

The Jurassic–Cretaceous boundary in the Tethys (= the Berriasian Stage base), located near the *Calpionella* Zone base roughly corresponds to middle part of Chron M19n and middle part of *Craspedites taimyrensis* Zone in Panboreal Superrealm. In Boreal areas, the Jurassic–Cretaceous boundary (the Ryazanian base) has been determined earlier at the base of *Chetaites sibiricus* Zone in the Nordvik section, this boundary is defined at the base of phosphate limestone 5 cm thick, enriched in iridium and other precious metals, (Zakharov et al., 1993) is now within Chron M18n. The detailed bio- and magnetostratigraphic data obtained for the Nordvik section (Anabar Bay, Laptev Sea coast) realized magnetochronologic calibration of the Jurassic–Cretaceous boundary beds in the Tethyan and Boreal areas.

### ACKNOWLEDGMENTS

The work was supported by the Russian Foundation for Basic Research, project nos. 03-05-64297 and 06-05-64284, Program no.14 of the Earthscience Division RAS, and by the GAČR agency, grant nos. 205-07-1365, 205-06-0842, MSM 0021620855. Private sponsorship by F. Shidlovsky and A. Zakharov should also be acknowledged. We warmly thank Dr. A.Yu. Guzhikov (Saratov State University, Russia) who became not merely reviewer but also scientific editor of paleo-

magnetic part in this paper, and second reviewer Dr. V.V. Mitta (Paleontological Institute of RAS, Russia).

Reviewers A.Yu. Guzhikov and V.V. Mitta

### REFERENCES

1. M. Chadima, P. Pruner, S. Šlechtá, et al., “Magnetic Fabric Variations in Mesozoic Black Shales, Northern Siberia, Russia: Possible Paleomagnetic Implications,” *Tectonophysics*, **418**, 145–162 (2006).
2. R. A. Fisher, “Dispersion on a Sphere,” *Proc. Soc. London, Ser. A*, **217**, 295–305 (1953).
3. V. Houša, M. Krs, M. Krsová, et al., “High-Resolution Magnetostratigraphy and Micropaleontology across the J/K Boundary Strata at Brodno near Zilina, Western Slovakia: Summary Results,” *Cretaceous Research*, **20**, 699–717 (1999).
4. V. Houša, M. Krs, O. Man, et al., “Detailed Magnetostratigraphy and Micropaleontology across the J/K Boundary Strata at Puerto Escaño, S. Spain,” in *25th General Assembly European Geophysical Society, 25–29 April, Nice, France. Research Abstracts (GRA)*, Vol. 2, 71 (2000).
5. V. Houša, M. Krs, O. Man, et al., “Combined Magnetostratigraphic, Paleomagnetic and Calpionellid Investigations Across Jurassic/Cretaceous boundary Strata in the Bosso Valley, Umbria, Central Italy,” *Cretaceous Research* **25**, 771–785 (2004).
6. J. Kirschvink, “The Least Squares Line and Plane and the Analysis of Paleomagnetic Data,” *Geoph. J. Royal Astr. Soc.*, **62**, 699–718 (1980).

7. D. N. Kiselev, "Sel'tso-Voskresenskoe," *Atlas of Geological Monuments of the Yaroslavl Oblast* (YaGPU, Yaroslavl, 2003), pp. 58–62.
8. O. Man, "A Comprehensive Interpretation of Magnetostratigraphic Data Based on the Pattern Recognition Technique," *Travaux Géophysiques*, No. XXXVIII, 74–75 (2006).
9. M. S. Mesezhnikov, "Tithonian, Volgian, and Portlandian Stages (Geological and Biological Events, Correlation)," in *Sedimentary Cover of the Earth. Stratigraphy and Paleontology* (Nauka, Moscow, 1989), pp. 100–107.
10. V. V. Mitta, "The Jurassic/Cretaceous Boundary: Continuation of Discussion," in *Proceedings of Scientific Conference on Paleontology, Biostratigraphy, and Paleogeography of the Boreal Mesozoic. Materials Session, Novosibirsk, April 26–28, 2006* (GEO, Novosibirsk, 2006), pp. 112–115.
11. J. Ogg and A. Smith, "The Geomagnetic Polarity Time Scale," in *Geologic Time Scale 2004*, Ed. by F. M. Gradstein, J. G. Ogg, and A. A. Smith (University Press, Cambridge, 2004), pp. 69–86.
12. S. A. Pisarevsky, *Paleomagnetic Directions and Pole Positions: Data for the USSR. Issue 5. Catalogue* (Soviet Geophysical Committee, World Data Center-B, Moscow, 1982).
13. G. A. Pospelova, *Paleomagnetic Directions and Pole Positions: Data for the USSR. Issue I. Catalogue* (Soviet Geophysical Committee, World Data Center-B, Moscow, 1971).
14. G. A. Pospelova, G. Y. Larionova, and A. V. Anuchin, "Paleomagnetic Investigations of Jurassic and Lower Cretaceous Sedimentary Rocks of Siberia," *Intern. Geol. Rev.* **10**, 1108–1118 (1968).
15. C. R. Scotese and J. Golonka, *Paleogeographic Atlas. PALEOMAP Progress Report 20-0682* (Department of Geology, University of Texas at Arlington, 1992).
16. N. I. Shul'gina, *Boreal Basins at the Jurassic–Cretaceous Boundary Interval* (Leningrad, Nedra, 1985).
17. V. A. Zakharov, S. L. Lapukhov, and O. V. Shenfil, "Iridium Anomaly at the Jurassic–Cretaceous Boundary in North Siberia," *Russ. J. Geol. Geophys.* **34** (1), 83–90 (1993).
18. V. A. Zakharov, T. I. Nal'nyaeva, and N. I. Shul'gina, "New Data on Biostratigraphy of Upper Jurassic and Lower Cretaceous Deposits on the Paksa Peninsula, the Anabar Embayment (North Central Siberia)," in *Paleobiogeography and Biostratigraphy of the Jurassic and Cretaceous of Siberia*, Ed. by V. A. Zakharov (Nauka, Moscow, 1983), pp. 56–99.
19. V. A. Zakharov and M. A. Rogov, "New Data on the Jurassic–Cretaceous Boundary Beds in Arctic (Nordvik Peninsula, North Siberia)," in *Proceedings of the 3rd All-Russian Meeting on "Cretaceous System in Russia and Adjacent Areas: Problems of Stratigraphy and Paleogeography," Saratov, September 26–30, 2006* (SO EAGO, Saratov, 2006), pp. 61–63 [in Russian].